Comparison of Different Approaches in Reflectarray Synthesis Based on Intersection Approach

Daniel R. Prado*, Jesús López-Fernández†, Manuel Arrebola†, Marcos R. Pino† and George Goussetis*
*Institute of Sensors, Signals and Systems, Heriot-Watt University, Edinburgh, U.K. Email: {dr38, g.goussetis}@hw.ac.uk
†Group of Signal Theory and Communications, Universidad de Oviedo, Spain. Email: {jelofer, arrebola, mpino}@uniovi.es

***Abstract*—This work presents a comparison between a number of numerical techniques for the copolar synthesis of reflectarray antennas. These techniques are based on the generalized intersection approach. The classical phase-only synthesis (POS) is considered using different methodologies to compute the gradient: the analytical approach by exactly calculating the derivative and two numerical methods based on finite differences, one using the FFT and another the technique of differential contributions (DFC). In addition, a direct layout optimization (DLO) for copolar synthesis is also considered. In order to make the DLO efficient, a surrogate model of the unit cell is employed. A computing time study is presented, showing that for copolar only synthesis at a single frequency, the POS technique using DFC has superior performance. Finally, a large reflectarray with European footprint for satellite broadcasting is synthesized, comparing the results obtained with all techniques.**

***Index Terms*—Reflectarray antenna, phase-only synthesis, numerical technique, differential contributions, contoured-beam, satellite broadcasting**

I. Introduction

Antenna pattern synthesis is important in any application that requires non-canonical patterns. It can be considered as the reverse of antenna analysis [1]: given a set of requirements on the radiated field, the antenna structure is sought. In practice, many of the antenna features are fixed beforehand and usually only the excitation is synthesized. In this regard, there are many techniques for the synthesis of antennas, including global and local search algorithms. For the case of reflectarray antennas, since they may be comprised of thousands of elements, local search, gradient-based algorithms are preferred [2], [3]. The computation of the gradient is the slowest operation, and thus it is interesting to provide solutions to accelerate computations. When possible, the best strategy is to analytically obtain the derivatives so computations are faster. However, there might be situations in which this is not possible, such as when performing the direct optimization of the layout [2]. Then, finite differences must be used, slowing computations.

In this work, we compare a number of techniques for the synthesis of reflectarray antennas. All of them are based on the use of the generalized intersection approach (IA) [1] and aim at improving its computational performance without losing accuracy. The baseline algorithm of [4] is considered, which employs finite differences to calculate the gradient and the FFT to efficiently obtain the far field. Then, the analytical derivative of the gradient is developed and compared with the baseline algorithm, showing superior computational performance. In addition, the technique of differential contributions [5] (DFC) to the far field is briefly introduced and considered in this study. Finally, support vector machines (SVMs) [6] are employed to perform a direct optimization of the layout to synthesize the required radiation pattern. Afterwards, a thorough computational study is carried out comparing all previous techniques to analyse their performance. Finally, they are applied to a large reflectarray for direct broadcast satellite (DBS) application with a European coverage, giving an overview of the performance of different approaches to synthesize reflectarrays.

This work was supported in part by the Ministerio de Ciencia, Innovación y Universidades under project TEC2017-86619-R (ARTEINE); by the Ministerio de Economía, Industria y Competitividad under project TEC2016-75103-C2-1-R (MYRADA); by the Gobierno del Principado de Asturias/FEDER under Project GRUPIN-IDI/2018/000191; by the Gobierno del Principado de Asturias through Programa "Clarín" de Ayudas Postdoctorales / Marie Curie-Cofund under project ACA17-09; by Ministerio de Educación, Cultura y Deporte / Programa de Movilidad "Salvador de Madariaga" (Ref. PRX18/00424).

II. Generalized Intersection Approach

The reflectarray synthesis is carried out using a local-search gradient-based algorithm known as generalized IA [1], which has been particularized for reflectarray phase-only synthesis (POS) in [4]. It is an iterative algorithm that performs two operations on the radiated field at each iteration:

$$\vec{E}_{i+1} = \mathcal{B}\left[\mathcal{F}\left(\vec{E}_i\right)\right], \tag{1}$$

where $\mathcal{F}$ is the forward projector, which computes the radiated field and then trims it according to some specifications given in the form of lower and upper masks; and $\mathcal{B}$ is the backward projector, which minimizes the distance between the current radiated field by the reflectarray and the field trimmed by the forward projector that complies with the specifications [3].

For the present case, a far field pattern synthesis is performed, and the generalized IA works with the squared field amplitude, or equivalently, the gain. We consider a single-offset reflectarray antenna (see Fig. 1) comprised of N elements and whose far field is computed at M points. Assuming that S variables are optimized, and denoting with $G_T(\vec{r})$ the trimmed gain by the forward projector, and with $G(\vec{r};\bar{\xi})$ the current gain pattern radiated by the reflectarray, the cost function which is minimized by the backward projector is [3]:

$$F(\vec{r};\bar{\xi}) = \sum_{m=1}^{M} \left\{ C(\vec{r}) \left[G_T(\vec{r}) - G\left(\vec{r};\bar{\xi}\right) \right] \right\}^2, \tag{2}$$

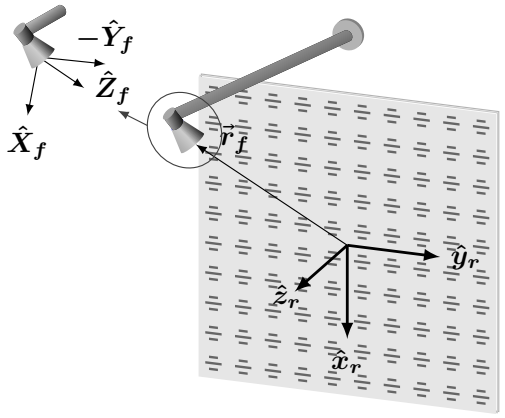

Fig. 1. Sketch of a single-offset reflectarray geometry.

where $\vec{r} \in \{\vec{r}_1, \ldots, \vec{r}_t, \ldots, \vec{r}_M\}$ is an observation point where the far field is computed; $C(\vec{r})$ is a weighting function and $\bar{\xi} = (\xi_1, \ldots, \xi_i, \ldots, \xi_S)$ is a vector of S optimization variables, which for the POS will be the phase-shift introduced by the reflectarray elements. The cost function in (2) is minimized by the Levenberg-Marquardt Algorithm (LMA), which requires the computation of the Jacobian matrix formed with the derivatives of the residuals:

$$R\left(\vec{r};\bar{\xi}\right) = C(\vec{r})\left(G_T(\vec{r}) - G\left(\vec{r};\bar{\xi}\right)\right). \tag{3}$$

Since we consider S optimizing variables, the LMA will require to compute S derivatives of (3).

III. Phase-Only Synthesis

A. Analytical Derivative

From here on, we drop the dependence on $\vec{r}$ to alleviate notation and to focus only on the optimization variables $\bar{\xi}$. Since for POS the optimization variables are the phase-shifts introduced by the reflectarray elements, there is an easy way to obtain the derivative analytically. For the computation of the Jacobian matrix (gradient), we need to obtain the following derivative:

$$R'_i\left(\bar{\xi}\right) = \frac{\partial R\left(\bar{\xi}\right)}{\partial \xi_i} = \frac{\partial\left[C \cdot \left(G_T - G(\bar{\xi})\right)\right]}{\partial \xi_i}. \tag{4}$$

where R is defined in (3) and R'_i indicates a partial derivative with respect to variable ξ_i. For the computation of the residual, the gain is proportional to the squared far field amplitude ($G \propto |E_{\text{ff}}\left(\bar{\xi}\right)|^2$). Thus, taking into account that $E_{\text{ff}}\left(\bar{\xi}\right)$ is complex, and that it can be written as the sum of its real and imaginary parts, using the chain rule it follows:

$$R'\left(\bar{\xi}\right) = -2\,C_2\left[E_{\text{ff,R}}\left(\bar{\xi}\right)E'_{\text{ff,R}}\left(\bar{\xi}\right) + E_{\text{ff,I}}\left(\bar{\xi}\right)E'_{\text{ff,I}}\left(\bar{\xi}\right)\right], \tag{5}$$

where $C_2 = 2\pi C/\eta_0 P_t$, $\eta_0 = \mu_0 c$ is the intrinsic impedance of vacuum and P_t the power radiated by the feed.

For the far field, we consider the copolar component in two linear polarizations, which are:

$$E^X_{\text{ff}}\left(\bar{\xi}\right) = E^X_{\text{CP}}\left(\bar{\xi}\right) = \cos\varphi E^X_\theta\left(\bar{\xi}\right) - \sin\varphi E^X_\varphi\left(\bar{\xi}\right), \tag{6a}$$

$$E^Y_{\text{ff}}\left(\bar{\xi}\right) = E^Y_{\text{CP}}\left(\bar{\xi}\right) = \sin\varphi E^Y_\theta\left(\bar{\xi}\right) + \cos\varphi E^Y_\varphi\left(\bar{\xi}\right). \tag{6b}$$

The superscript indicates the linear polarization of the feed (see Fig. 1). In addition, since the POS is done independently for each linear polarization, we will focus on polarization X. The steps for polarization Y will be identical. Thanks to the linearity of the differential operator, (5) can be written as:

$$\begin{aligned} R'\left(\bar{\xi}\right) = -2\,C_2\Big[&E^X_{\text{CP,R}}\left(\bar{\xi}\right)\left(\cos\varphi E'_{\theta,R}\left(\bar{\xi}\right) - \sin\varphi E'_{\varphi,R}\left(\bar{\xi}\right)\right) \\ &+ E^X_{\text{CP,I}}\left(\bar{\xi}\right)\left(\cos\varphi E'_{\theta,I}\left(\bar{\xi}\right) - \sin\varphi E'_{\varphi,I}\left(\bar{\xi}\right)\right)\Big] \end{aligned} \tag{7}$$

For POS, the far field in spherical coordinates for polarization X are [4]:

$$\begin{aligned} E^X_\theta\left(\bar{\xi}\right) = A\Big[&P^X_x\left(\bar{\xi}\right)\cos\varphi - \eta_0\cos\theta\big(Q^X_x\left(\bar{\xi}\right)\sin\varphi - \\ &Q^X_y\left(\bar{\xi}\right)\cos\varphi\big)\Big], \end{aligned} \tag{8a}$$

$$\begin{aligned} E^X_\varphi\left(\bar{\xi}\right) = -A\Big[&P^X_x\left(\bar{\xi}\right)\sin\varphi\cos\theta + \eta_0\big(Q^X_x\left(\bar{\xi}\right)\cos\varphi + \\ &Q^X_y\left(\bar{\xi}\right)\sin\varphi\big)\Big], \end{aligned} \tag{8b}$$

where the subscript in P and Q indicate the component of the field with regard to the reflectarray coordinate system (see Fig. 1), and $A = jk_0\exp\left(-jk_0 r\right)/4\pi r$. At this point, A is a complex number, as well as the spectrum functions P and Q. Since we need the real and imaginary parts of (8), it seems that we need to consider the multiplication of A with P and Q. However, A is a common factor to all equations and does not depend on the optimization variables. Thus, we can extract it from (8) and add it to C_2 in (5) so the following operations are simplified. With that, the real and imaginary parts of E_θ are:

$$\begin{aligned} E^X_{\theta,R}\left(\bar{\xi}\right) = \cos\varphi P^X_{x,R}\left(\bar{\xi}\right) - \eta_0\cos\theta\sin\varphi Q^X_{x,R}\left(\bar{\xi}\right) + \\ \eta_0\cos\theta\cos\varphi Q^X_{y,R}\left(\bar{\xi}\right), \end{aligned} \tag{9a}$$

$$\begin{aligned} E^X_{\theta,I}\left(\bar{\xi}\right) = \cos\varphi P^X_{x,I}\left(\bar{\xi}\right) - \eta_0\cos\theta\sin\varphi Q^X_{x,I}\left(\bar{\xi}\right) + \\ \eta_0\cos\theta\cos\varphi Q^X_{y,I}\left(\bar{\xi}\right). \end{aligned} \tag{9b}$$

And similarly for E^X_φ.

For the computation of the derivatives of the real and imaginary parts of E^X_θ and E^X_φ, we need to compute the derivatives of the real and imaginary parts of the spectrum functions P and Q, by virtue of the linear property of the differential operator. For instance, a generic spectrum function P takes the form:

$$P\left(\bar{\xi}\right) = K\sum_{l=1}^{N}\exp\left(j\xi_l\right)E_{\text{inc},l}\exp\left(jk_0(ux_l + vy_l)\right), \tag{10}$$

where $K \in \mathbb{R}$ is the amplitude of the element pattern, $E_{\text{inc},l}$ is the complex incident field on reflectarray element l and ξ_l the phase-shift introduced by that element, which is the optimization variable for the POS. After extracting the real and imaginary parts of (10), we have:

$$\begin{aligned} P_R\left(\bar{\xi}\right) = K\sum_{l=1}^{N}\Big[&\cos\xi_l\,E_{\text{inc},l,R}\,\cos k_l - \sin\xi_l\,E_{\text{inc},l,I}\,\cos k_l - \\ &\cos\xi_l\,E_{\text{inc},l,I}\,\sin k_l - \sin\xi_l\,E_{\text{inc},l,R}\,\sin k_l\Big], \end{aligned} \tag{11a}$$

$$P_I\left(\bar{\xi}\right) = K\sum_{l=1}^{N}\Big[\cos\xi_l\, E_{\text{inc},l,R}\,\sin k_l - \sin\xi_l\, E_{\text{inc},l,I}\,\sin k_l + \cos\xi_l\, E_{\text{inc},l,I}\,\cos k_l + \sin\xi_l\, E_{\text{inc},l,R}\,\cos k_l\Big], \tag{11b}$$

where $k_l = k_0(ux_l + vy_l)$. Thus, the derivative for any element $l = i$ is:

$$P'_{i,R}\left(\bar{\xi}\right) = -K\Big[\sin\xi_i\, E_{\text{inc},i,R}\,\cos k_i + \cos\xi_i\, E_{\text{inc},i,I}\,\cos k_i - \sin\xi_i\, E_{\text{inc},i,I}\,\sin k_i + \cos\xi_i\, E_{\text{inc},i,R}\,\sin k_i\Big], \tag{12a}$$

$$P'_{i,I}\left(\bar{\xi}\right) = -K\Big[\sin\xi_i\, E_{\text{inc},i,R}\,\sin k_i + \cos\xi_i\, E_{\text{inc},i,I}\,\sin k_i + \sin\xi_i\, E_{\text{inc},i,I}\,\cos k_i - \cos\xi_i\, E_{\text{inc},i,R}\,\cos k_i\Big]. \tag{12b}$$

The derivatives in (12) can be used for the four cases $P^{X/Y}_{x/y}$ by simply using the adequate incidence field. For instance, the spectrum function P^X_y would need the field $E^X_{\text{inc},y}$. For the spectrum functions Q, which use the magnetic field [4], a similar process is carried out, yielding similar derivatives as in (12). Finally, as it can be seen, the computation of the derivative only considers the contribution of the element depending on variable ξ_i, and thus the time complexity of computing one derivative analytically is $\mathcal{O}(M)$.

B. Derivative using Finite Differences with the FFT

A widely employed numerical method for the computation of derivatives are finite differences. In this way, (4) may be expressed, e.g., using the backward lateral difference [7]:

$$R'_i = \frac{R(\bar{\xi}) - R(\bar{\xi} - h\hat{e}_i)}{h} + \mathcal{O}(h), \tag{13}$$

where h is a small positive scalar [7] and $\hat{e}_i$ the ith unit vector. The term $R(\bar{\xi})$ is common to all derivatives, while the other term, $R(\bar{\xi} - h\hat{e}_i)$, is computed for each derivative.

For the computation of the residual, the far field is computed using the first principle of equivalence in electromagnetics [8], which requires the computation of the electric and magnetic spectrum functions. They may be expressed as a 2-D Inverse Discrete Fourier Transform (IDFT2) of the electromagnetic reflected tangential field, which is efficiently evaluated by the FFT algorithm [3]. The electric reflected tangential field is:

$$\vec{E}^{X/Y}_{\text{ref}}(x_i, y_i) = \mathbf{R}_i \cdot \vec{E}^{X/Y}_{\text{inc}}(x_i, y_i), \tag{14}$$

with E_{inc} the incident field impinging from the feed and

$$\mathbf{R}_i = \begin{pmatrix} \rho_{xx,i} & \rho_{xy,i} \\ \rho_{yx,i} & \rho_{yy,i} \end{pmatrix} \tag{15}$$

is the matrix of reflection coefficients. The reflected tangential magnetic field is obtained from $\vec{E}_{\text{ref}}$ assuming a locally incident plane wave [3]. Finally, in POS (15) is simplified assuming no losses ($|\rho_{xx}| = |\rho_{yy}| = 1$) and no cross-polarization ($\rho_{xy} = \rho_{yx} = 0$):

$$\mathbf{R}_i = \begin{pmatrix} \exp\left(j\xi_{xx,i}\right) & 0 \\ 0 & \exp\left(j\xi_{yy,i}\right) \end{pmatrix}, \tag{16}$$

where $\xi_{xx,i}$ and $\xi_{yy,i}$ are the phase-shift introduced by the element for polarization X and Y, respectively.

Using this methodology, the time complexity of computing the derivative is approximately $\mathcal{O}\left(M \log M\right)$ due to the use of the FFT.

C. Numerical Derivative using Differential Contributions

An alternative numerical method for the computation of the gradient is the DFC technique [5]. It is based on the linearity of Maxwell's equations. This property provides a linear relation between the tangential field at the aperture (14) and the radiated field. In this way, each derivative expressed with finite differences in the form of (13) can be efficiently computed by only taking into account the differential contribution of the reflectarray element depending on variable ξ_i. Thus, for the derivative calculation, the time complexity of computing the far field is reduced from $\mathcal{O}(M \log M)$ when using the FFT to $\mathcal{O}(M)$ using the DFC technique. This time complexity is the same as for the analytical derivative.

For a thorough mathematical description, the reader is referred to [5], where the DFC technique is detailed for both far field and near field. In this work, the DFC is applied for a far field pattern synthesis.

IV. Direct Layout Synthesis

Another approach for the synthesis of reflectarray antennas is to perform a direct layout synthesis (DLS). For instance, in [3] a method of moments based on local periodicity (MoM-LP) was employed to analyse the reflectarray element and obtain its electromagnetic response in the form of the reflection coefficient matrix of (15). However, using MoM-LP results in slow computations. There are several approaches to accelerate this analysis, including the use of artificial neural networks [9], support vector machines (SVMs) [6] or databases [2]. They require the use of a full-wave analysis of the unit cell to generate samples of the reflection coefficients, but this operation is only performed once and the samples can be reused for multiple designs. Here, we have opted to employ the SVM described in [6].

The main difference between a POS and a DLS is the computation of the $\mathbf{R}_i$ matrix. For POS, the matrix is simplified as shown in (16), while a DLS uses the full matrix in (15). Let $\rho_{R,I}$ be the real or imaginary part of any reflection coefficient of (15). Then, the SVM provides an estimation of $\rho_{R,I}$ as:

$$\tilde{\rho}_{R,I}(\vec{x}) = \sum_{k=1}^{N_s}\left[\left(\alpha_k^- - \alpha_k^+\right) K_e(\vec{x_k}, \vec{x})\right] + b, \tag{17}$$

where $\vec{x}$ is the vector with geometrical features of the unit cell used as variables for the training; $\vec{x_k}$ is the kth support vector; N_s is the number of support vectors; α_k^- and α_k^+ are the kth optimal Lagrange multipliers; b is the offset; and K_e is the kernel function, which in this case is a Gaussian function [6]. Thus, each reflection coefficient is expressed with the SVM as a linear combination of N_s Gaussian functions.

Since the use of SVMs only deals with the computation of the reflection coefficient matrix, the previously described techniques may be used for the computation of the gradient. However, the analytical derivative is cumbersome to obtain, so

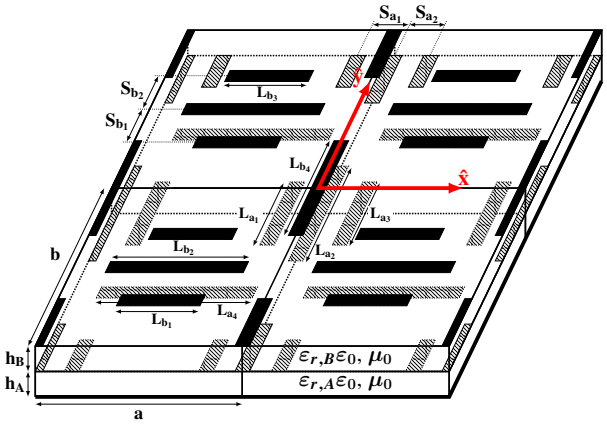

Fig. 2. Reflectarray unit cell consisting of two layers of parallel and coplanar dipoles divided in two sets of four dipoles per linear polarization.

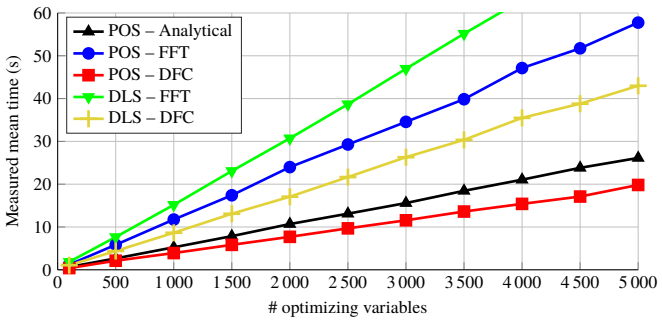

Fig. 3. Measured computing time of the Jacobian matrix computation with different methods: analytical derivative (black), finite differences with FFT (blue) and finite differences with DFC (red) for phase-only synthesis; and direct layout synthesis (DLS) with the FFT (green) and with DFC (yellow).

only finite differences with FFT and DFC will be employed. For the first case, the time complexity of computing the derivative is $\mathcal{O}(N_s + M \log M)$ while for the second case it is $\mathcal{O}(N_s + M)$.

V. Results for the Gradient Computation

A. Specifications

A thorough computational study was performed to compare the techniques described previously. Simulations were carried out in a computer with an Intel Core i7-7700 CPU at 3.60 GHz. In addition, computations are fully parallelized, computing one derivative per available thread. Also, the grid in which the far field is obtained with the FFT has 512×512 points.

For the DLS with the SVM, a unit cell geometry must be specified. In particular, the reflectarray element shown in Fig. 2 is employed. It consists of two sets of parallel and coplanar dipoles in two layers of metallization. Each set of four dipoles controls the phase-shift for a linear polarization. For the present case, only the lengths of the dipoles are considered as optimizing variables. Moreover, they are reduced from eight variables per element to two using the following relations [10]:

$$\begin{aligned} &L_{a_4} = T_x \;\; ; \;\; L_{b_1} = L_{b_3} = 0.63\,T_x \;\; ; \;\; L_{b_2} = 0.93\,T_x, \\ &L_{b_4} = 0.95\,T_y \;\; ; \;\; L_{a_1} = L_{a_3} = 0.58\,T_y \;\; ; \;\; L_{a_2} = T_y. \end{aligned} \tag{18}$$

Thus, only T_x and T_y will be considered when training the SVM following the guidelines presented in [6] and when performing the DLS in this work. Following this approach, the vector $\vec{x}$ in (17) is $\vec{x} = (T_x, T_y)$.

The rest of the parameters of the unit cell are fixed, including the working frequency at 11.85 GHz, periodicity $a = b = 14\,\text{mm}$, the width of the dipoles is 0.5 mm, the separation between dipoles is $S_a = S_b = 4\,\text{mm}$, the substrate for the bottom layer has a height of $h_A = 2.363\,\text{mm}$ and a complex permittivity of $\varepsilon_{r,A} = 2.55 - 2.295 \cdot 10^{-3}$, while the top layer has a height of $h_B = 1.524\,\text{mm}$ and a complex permittivity of $\varepsilon_{r,B} = 2.17 - 1.953 \cdot 10^{-3}$.

B. Numerical Results

The baseline scenario corresponds to the algorithm presented in [4], using the POS with finite differences to calculate the derivatives and the FFT to efficiently compute the radiation patterns as described in Section III.B. It corresponds to the blue line in Fig. 3. The POS may be improved by analytically calculating the derivatives, which in principle would provide the optimal scenario. Indeed, computing time using the analytical derivative improve those of the finite differences using the FFT by around 54%, as it can be seen in Fig. 3 comparing the blue and black lines. However, when using the DFC technique for the computation of the derivatives in POS, it offers faster computations than the analytical derivative. In fact it is around 66% faster than when using the FFT and 27% faster than the analytical derivative. The latter is possible due to the fact that, although both techniques present the same time complexity for the computation of the derivative, $\mathcal{O}(M)$, the DFC has less operations in the loop sweeping all points where the radiation pattern is computed.

The DLS using the SVMs is a slightly different scenario, although it was tested in the same conditions as the POS. Now, the optimizing variables are not the required phase-shift, but the length of the dipoles of the chosen unit cell. In addition, the use of the SVMs requires additional computation to obtain the reflection coefficient matrix. Thus, time cost is higher than for POS. This is evident when using the SVM to analyse the reflectarray element and using the FFT in the computation of the radiation pattern with finite differences (green line). However, when the DFC is used together with the SVM (yellow line), computations are faster than the POS using FFT, even though using the SVM a direct optimization is carried out.

C. Discussion

From the results shown in Fig. 3 it is clear that the POS with DFC is the best strategy to carry out copolar synthesis in reflectarray antennas. The result of this synthesis is a phase-shift distribution for each reflectarray element. The following step would be to adjust, element by element, its dimensions so they produce the required phase-shift. This is done by using a

zero-finding routine [11] and it may take a significant amount of time if using a MoM-LP tool, but using SVMs it only takes a few seconds for very large reflectarrays comprised of thousands of elements [12].

On the other hand, using SVM to carry out a copolar synthesis is slower than POS when using the DFC technique. Although using the SVM for the synthesis directly provides the reflectarray layout and thus there is no need to further adjust the element dimensions, as it is the case for POS, it is still slower than carrying out a POS since the reflectarray design using SVM is very fast [12], in the order of seconds. Thus, in light of the previous results, the best strategy to carry out a copolar synthesis at a single frequency is a POS with the DFC technique, in light of the results shown in Fig. 3.

VI. Copolar Synthesis of a Large Reflectarray for Contoured-Beam Application

A. Antenna specifications

The considered reflectarray is elliptical and comprised of 4068 elements in a regular grid with 74×70 elements in the main axes. The working frequency is 11.85 GHz and the periodicity is $14\,\text{mm} \times 14\,\text{mm}$, which is $0.553\lambda_0$. The feed phase center is placed at $\vec{r}_f = (-358, 0, 1.070)\,\text{mm}$ with respect to the center of the reflectarray (see Fig. 1). For the feed, an ideal model based on a $\cos^q\theta$ function is employed, with $q = 23$ generating an illumination taper of $-18.5\,\text{dB}$. The antenna is placed in a satellite in geostationary orbit at 10° E longitude. The same coverage as in [13] is considered, where Europe is divided into two zones. The interior area (zone 1) presents a copolar specification of 28.5 dBi while the exterior area (zone 2) has a copolar requirement of 25.5 dBi. The coverage requirements take into account typical satellite pointing errors: 0.1° in roll and pitch, and 0.5° in yaw.

B. Phase-Only Synthesis

The starting point for the POS is a phase-shift distribution that generates a pencil beam pattern pointing at $(\theta, \varphi) = (16.6°, 0°)$, which is approximately the center of zone 1 of the European footprint. After the POS, the synthesized phase-shift was compared with the one obtained using the DFC and the FFT, and the differences are shown, respectively, in Fig. 4(a) and Fig. 4(b). As it can be seen, the differences after 255 gradient evaluations using different numerical techniques is very low. In fact, for Fig. 4(a) the mean absolute deviation (MAD) is only 0.14°, while for Fig. 4(b) is 1.82°.

Fig. 5 shows the copolar and crosspolar patterns for polarization X obtained for the POS carried out with the three techniques. As it can be seen, the little differences in phase shift shown in Fig. 4 lead to virtually the same radiation patterns. In fact, the minimum copolar gain for zone 1 is 29.34 dBi for the three cases, while for zone 2 is 26.29 dBi for the analytical derivative and DFC technique, and 26.28 dBi for the FFT: a difference of only 0.01 dBi, due to the larger difference in the final obtained phase-shifts, but still negligible. The crosspolar pattern was also obtained, simulating the three designed reflectarrays with a MoM-LP [14]. The simulated

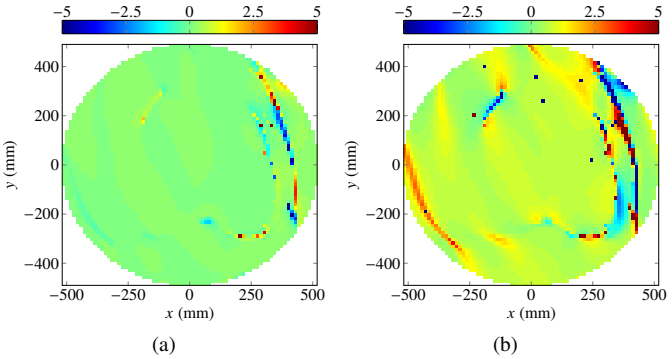

(a) (b)

Fig. 4. Phase difference in degrees (°) between the far field syntheses carried out computing the gradient with analytical derivatives and using finite differences with (a) the DFC technique and (b) using the FFT.

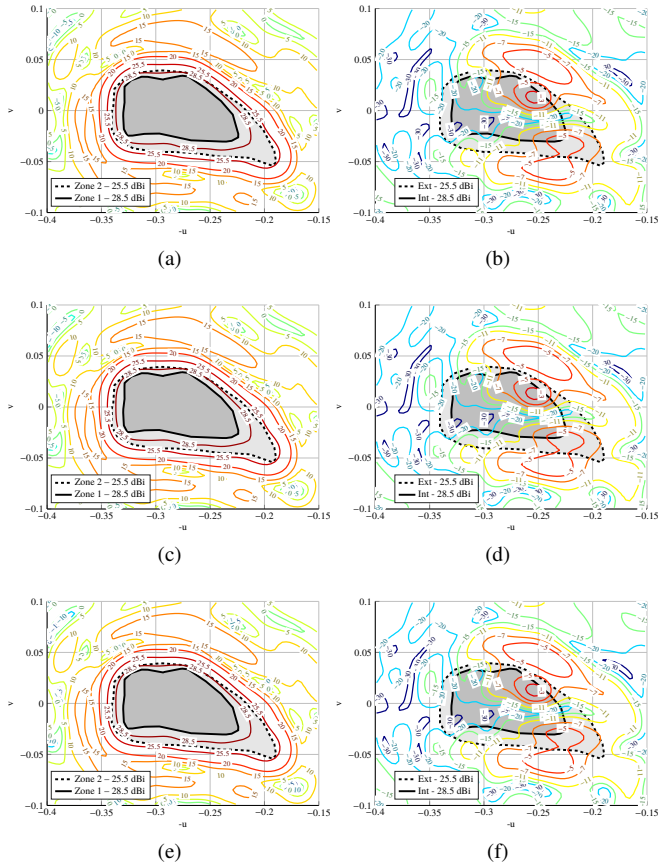

(a) (b)

(c) (d)

(e) (f)

Fig. 5. (a), (c), (e) Copolar and (b), (d), (f) crosspolar patterns for polarization X in gain (dBi) of the synthesized European footprint obtained with (a), (b) analytical derivatives, (c), (d) the DFC technique and (e), (f) the FFT.

crosspolar patterns are very similar. The maximum difference is 0.02 dB when comparing the different crosspolar patterns.

C. Direct Layout Synthesis

A DLS for copolar synthesis using SVMs was also carried out for polarization X. Now, the optimizing variables are no longer the phase-shifts introduced by the reflectarray elements, but the lengths of the dipoles (T_x and/or T_y). Thus, the

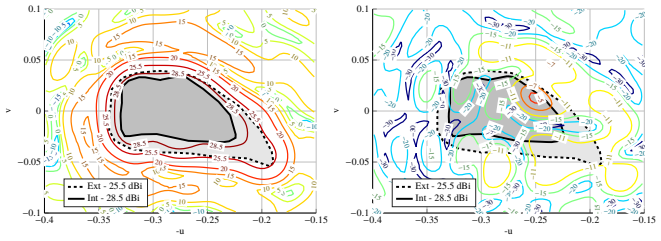

(a) (b)

Fig. 6. For the Direct Layout Synthesis, obtained (a) copolar and (b) crosspolar patterns for polarization X.

search space which the algorithm has to navigate is completely different. In addition, since the SVM models the full matrix of reflection coefficients in (15), it includes the losses of the substrate, which are not taken into account in the POS.

The optimization was carried out with the SVM using the DFC technique. The copolar and crosspolar pattern were simulated, after the synthesis with SVM, using the MoM-LP of [14] and the radiation patterns of Fig. 6 were obtained. For the copolar pattern, zone 1 presents a minimum gain of 29.32 dBi while zone 2 has a minimum gain of 26.06 dBi. Both are slightly lower than the POS. However, if a layout is obtained from the phase-shift obtained with POS including the losses, zone 1 presents a minimum gain of 29.25 dBi while for zone 2 is 26.18 dBi. Thus, the results of a DLS and a POS plus a design to obtain the layout are similar. In any case, the patterns are very similar in the four cases.

VII. Conclusions

This work has presented a thorough comparison between a number of numerical methods for the synthesis of reflectarray antennas using the generalized intersection approach (IA) algorithm. The generalized IA is a gradient-based local search algorithm. For a POS, three numerical techniques are considered: the computation of the derivatives with finite differences using the FFT, the technique of differential contributions (DFC) and the analytical derivative. Support vector machines (SVMs) were also considered for a direct synthesis of the reflectarray using finite differences with FFT and DFC. The equations show that the time complexity of the DFC technique is the same as the analytical derivative, while the use of the FFT is the slowest. A numerical study shows that the use of the DFC technique is 27% faster than the analytical derivative and 66% faster than the baseline scenario using the FFT for the computation of the far field. Regarding the direct layout optimization, the overhead of the SVM computations to obtain the full matrix of reflection coefficients makes this approach slower than the other two, specially when using the FFT. However, the combination of SVM plus the DFC technique provides faster computations than the baseline scenario, while directly obtaining the final reflectarray layout.

Finally, the techniques were applied in the same conditions to the synthesis of a very large reflectarray for DBS application with a European footprint with two coverage zones having different gain requirements. The results obtained with the analytical derivative are considered as reference. It has been shown that the synthesized phase-shifts with the three methods are very similar, with a mean absolute deviation of just 0.14° when using the DFC technique and 1.82° when using the FFT. Regarding the direct layout synthesis, the results in the antenna performance are very similar to those obtained with the POS after the layout is obtained to take into account the losses of the substrate.

For single frequency optimization it can be concluded that the best approach for reflectarray synthesis is to employ a phase-only synthesis with the differential contributions technique and use SVM in a later stage to obtain the final layout or improve other parameters of the antenna.

References

[1] O. M. Bucci, G. D'Elia, G. Mazzarella, and G. Panariello, "Antenna pattern synthesis: a new general approach," *Proc. IEEE*, vol. 82, no. 3, pp. 358–371, Mar. 1994.

[2] M. Zhou, S. B. Sørensen, O. S. Kim, E. Jørgensen, P. Meincke, and O. Breinbjerg, "Direct optimization of printed reflectarrays for contoured beam satellite antenna applications," *IEEE Trans. Antennas Propag.*, vol. 61, no. 4, pp. 1995–2004, Apr. 2013.

[3] D. R. Prado, M. Arrebola, M. R. Pino, R. Florencio, R. R. Boix, J. A. Encinar, and F. Las-Heras, "Efficient crosspolar optimization of shaped-beam dual-polarized reflectarrays using full-wave analysis for the antenna element characterization," *IEEE Trans. Antennas Propag.*, vol. 65, no. 2, pp. 623–635, Feb. 2017.

[4] D. R. Prado, M. Arrebola, M. R. Pino, and F. Las-Heras, "Improved reflectarray phase-only synthesis using the generalized intersection approach with dielectric frame and first principle of equivalence," *Int. J. Antennas Propag.*, vol. 2017, pp. 1–11, May 2017.

[5] D. R. Prado, A. F. Vaquero, M. Arrebola, M. R. Pino, and F. Las-Heras, "Acceleration of gradient-based algorithms for array antenna synthesis with far field or near field constraints," *IEEE Trans. Antennas Propag.*, vol. 66, no. 10, pp. 5239–5248, Oct. 2018.

[6] D. R. Prado, J. A. López-Fernández, G. Barquero, M. Arrebola, and F. Las-Heras, "Fast and accurate modeling of dual-polarized reflectarray unit cells using support vector machines," *IEEE Trans. Antennas Propag.*, vol. 66, no. 3, pp. 1258–1270, Mar. 2018.

[7] J. Nocedal and S. J. Wright, *Numerical Optimization*, 2nd ed. New York, NY, USA: Springer, 2006.

[8] W. L. Stutzman and G. A. Thiele, *Antenna Theory and Design*, 3rd ed. Hoboken, NJ, USA: John Wiley & Sons, 2012.

[9] A. Freni, M. Mussetta, and P. Pirinoli, "Neural network characterization of reflectarray antennas," *Int. J. Antennas Propag.*, vol. 2012, pp. 1–10, May 2012.

[10] J. A. Encinar, R. Florencio, M. Arrebola, M. A. Salas-Natera, M. Barba, J. E. Page, R. R. Boix, and G. Toso, "Dual-polarization reflectarray in Ku-band based on two layers of dipole arrays for a transmit-receive satellite antenna with South American coverage," *Int. J. Microw. Wirel. Technol.*, vol. 10, no. 2, pp. 149–159, 2018.

[11] J. Huang and J. A. Encinar, *Reflectarray Antennas*. Hoboken, NJ, USA: John Wiley & Sons, 2008.

[12] D. R. Prado, J. A. López-Fernández, M. Arrebola, and G. Goussetis, "Support vector regression to accelerate design and crosspolar optimization of shaped-beam reflectarray antennas for space applications," *IEEE Trans. Antennas Propag.*, vol. 67, pp. 1659–1668, Mar. 2019.

[13] J. A. Encinar, L. S. Datashvili, J. A. Zornoza, M. Arrebola, M. Sierra-Castaner, J. L. Besada-Sanmartin, H. Baier, and H. Legay, "Dual-polarization dual-coverage reflectarray for space applications," *IEEE Trans. Antennas Propag.*, vol. 54, no. 10, pp. 2827–2837, Oct. 2006.

[14] R. Florencio, R. R. Boix, and J. A. Encinar, "Enhanced MoM analysis of the scattering by periodic strip gratings in multilayered substrates," *IEEE Trans. Antennas Propag.*, vol. 61, no. 10, pp. 5088–5099, Oct. 2013.